3-Axis accelerometer and strain sensor readout for MEMS-based capacitive sensors

J.M. Santana, R.A.T. van den Hoven, C.A.P van Liempd

WATS-Low Power Analog Interfaces, imec-Holst Centre, Eindhoven 5656AE, The Netherlands

Abstract

A low-power capacitive readout for MEMS-based strain sensors and accelerometers is presented. A novel technique to optimise the trade-off between gain, bandwidth and noise is introduced. The readout can work with both types of sensors in the range of ±2.5g and ±20,000 με. Artefact cancellation such as residual motion is suppressed due to accurate control of the 3dB point in the built-in filter of the architecture. A figure of merit of 4.41×10^{-20} F√(W/Hz) was achieved. The ASIC was developed using a 0.25μm CMOS technology.

Keywords: capacitive readout, Signal-to-noise ratio, low-power.

1. System requirements

Low power and versatility are key demands for readout architectures for accelerometers and strain sensors that require minimum maintenance. Battery operated systems with an average of several years autonomy are a must in several applications such as healthcare and construction. Versatile systems that can work with several types of sensors with very little or no extra redesign or dedicated architectures are more and more in demand.

For the MEMSCON project an architecture which can handle MEMS-based comb-finger capacitive strain sensors and accelerometers is a must. The same architecture should be able to readout signals from half-bridge variable capacitors with different nominal capacitances, parasitics (internal and external) and working principle. A dedicated architecture for the accelerometer and another one for the strain sensor represents extra die area, complexity, power consumption and extra costs, therefore the need for a single readout architecture that can handle both types of devices.

The desired architecture should be able to work in the range of ±2.5g and ±20,000 με for the accelerometer and the strain sensor respectively with accuracies of 1mg and 10 με. For the accelerometer a bandwidth of 100Hz is required. The current consumption should be in the range of 100μA and the area of the ASIC less than 16mm^2. Artefacts such as residual motion, common in MEMS-based comb-fingers devices, should be suppressed.

1.1 Readout architectures and sensors

State-of-the-art readout architectures are based on commonly known techniques such as modulation-demodulation of signals, switched capacitors and Sigma-Delta [2,3]. Open-loop and closed-loop architectures are common in commercially available devices. Nevertheless power consumption is still a concern and, except for dedicated architectures developed for a specific type of sensor, its values are still high in the range of hundreds of microwatts to miliwatts. There are several reports in the literature which show the optimization of power consumption for a certain bandwidth range, noise and power but with the drawback of only being able to handle a sensor which is tailor made to achieve a good trade-off of such parameters.

MEMS-based comb finger devices in a half-bridge configuration produce a charge/capacitance change when a lateral or vertical displacement of the finger occurs [1]. The principle of operation of these two options is different; namely in the first one capacitance is proportional to the area of the overlapping fingers and the second is inversely proportional to the distance between the fingers. These modes of operation lead to different readout architectures and design specifications. In the case of a strain sensor the signal is mainly a DC one whereas for the accelerometer the signal is AC. The actuation voltages for the sensors can vary from a few tenths of a volt to volts. Usually split supplies are required to actuate the sensors so to match the reference voltage of the front-end of the readout.

Artefacts like residual motion [4,5] can produce spurious accelerations that cannot be distinguished at the input of the readout and in some cases can have values high enough to interfere with the performance of the ASIC by lowering its resolution, which may be critical for applications such as earthquake sensing.

1.2 Proposed architecture

A novel architecture with the system demands was developed which, could readout MEMS-based comb finger on a half-bridge configuration for either accelerometers or strain sensors with a wide range of specifications with no extra customization or redesign.

The diagram shown in Figure 1 shows the proposed architecture.

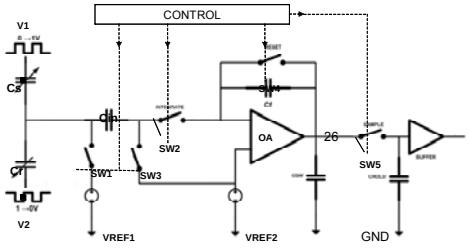

Fig. 1. Single-channel readout architecture.

It consists of a charge amplifier (OTA) with a capacitor C_f that is set to a certain gain and capacitor CBW to control the bandwidth of the amplifier. The accelerometer and/or the strain sensor are depicted as a pair of two variable capacitors on the left of the diagram. Between the common node of the sensor and the inverting input of the OTA a capacitor C_1 is placed which decouples the sensor from the readout circuit. This feature allows the architecture to handle a wide range of sensor specifications such as maximum actuation voltage, which produces an electric field on the fingers that if high enough can cause sticking or permanent damage.

At each side of the capacitor C_1 there are switches connected to voltage references V_{REF1} and V_{REF2}. These references set the voltage at the common node of the half-bridge and at the non-inverting input of the amplifier allowing for more versatility in the bias voltages of the OTA and those of the sensor. In this case study a 1.0V actuation voltage is required for the accelerometer and a 3.0V supply for the amplifier. With the proposed architecture the voltages on the sensor and on the amplifier can be set independently.

The architecture allows integrating a pre-specified number of charge pulses. The charge from the sensor goes through C_1 and is integrated in C_f . This appears as voltage at the output of the amplifier. The principle is shown in Figure 2. The number of integrated pulses sets the gain of the system in comparison with conventional designs [2,9]. At every rising/falling edge of the actuation voltage a charge/current pulse is created. The positive (or negative) pulses are then integrated in C_f, sampled and held at the output of the amplifier. In the case of the accelerometer a 3-axis system is required, therefore 3 channels are multiplexed in a sequence that allows to read X, Y and Z.

For the strain sensor application only one channel is used and read. In this case the signal is not multiplexed and can be measured as a simple DC value which is proportional to the applied stress.

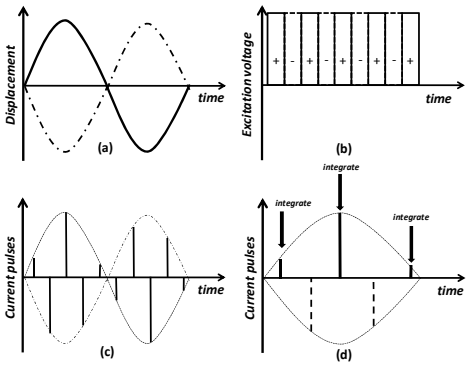

Fig. 2. Variable capacitor electrical model results (a) Proof-mass displacement at the input of the model (b) actuation voltages (c) current pulses at output of half-bridge (d) only positive pulses are integrated.

The timing sequence of the readout is shown in Figure 3. Between the Sample and Reset signals a number of pulses are sent to integrate capacitor C_f.

The ASIC also supplies synchronization signals which tell the user when the (for accelerometer X, Y and Z) values are available to be read.

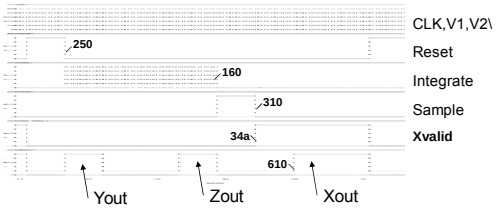

Fig. 3. Timing sequence of the readout.

The duty cycle of the integration pulses can also be varied allowing for more versatility in the gain of the system as well as the trade-off between gain and integrated noise. The width of the Sample and Reset signals can also be varied as well to suit specific demands of the end-users.

The readout was fabricated on a 0.25µm CMOS technology with M-i-M capacitors. The amplifier is a standard OTA as described in common literature. Special care was taken to minimize the Input-referred-noise of the differential stage so to reduce the 1/f noise if the transistors to a level that will not hinder the performance of the front-end.

2. Results

2.1 Dynamic and static measurements

The measurement results for the accelerometer and strain sensor devices are shown in the next figures. Figure 4 shows the output voltage for a 20Hz sine-wave input applied to the readout with a shaker. A range of ±2.5g was achieved with a nonlinearity of less than 1%. As can be seen in the plot the X, Y and Z signals appear in the desired sequence.

The sensitivity of the readout was varied by setting the number of integrated pulses to 2x, 4x, 8x and 16x the original value (24 pulses). The results are shown in Figure 5. The gain increases linearly as the number of pulses increase.

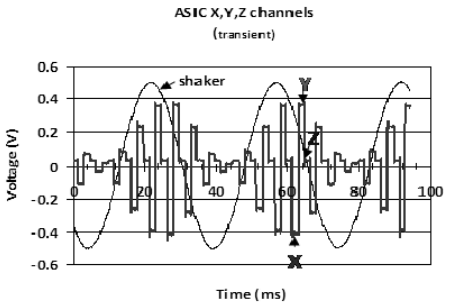

Fig. 4. Output voltage of the readout for a 20Hz sine-wave input signal.

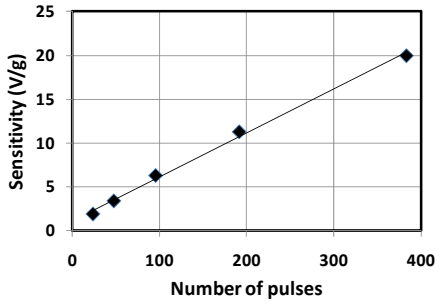

Fig. 5. Variable sensitivity of the readout as function of number of integrated pulses.

As for the strain sensor, the measurements results are shown in Figure 6. A range of ±20,000 με was achieved with linearity better than 0.6%. As seen in the plot the middle point corresponds to 1.25V (also in the case of the accelerometer) which was set by the reference voltage V_{REF2}.

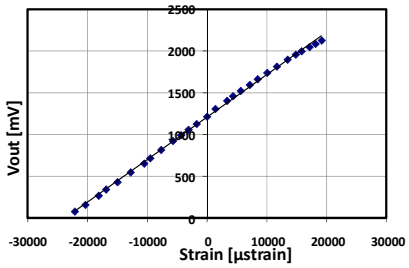

Fig. 6. Strain sensor measurements.

2.2 Noise measurements

To assess the noise performance of the system a series of noise measurements were taken. The readout was placed in the shaker and its output connected to a spectrum analyser. Several frequencies in the range of the accelerometer application were recorded. Figure 7 shows the results for a 70Hz input signal.

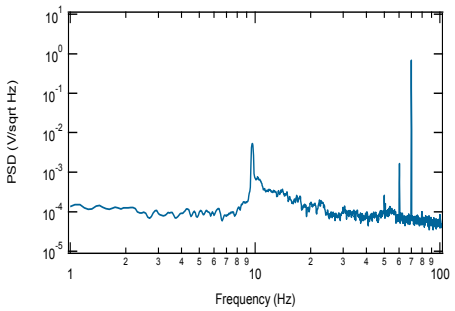

Fig. 7. PSD of the readout for a 70Hz input sine-wave.

As seen in the previous figure a clean output signal is obtained. The signal is equivalent to a 13-bit resolution, which makes the system easily compatible with several commercial ADC converters if the signal is to be digitised.

In order to determine the Signal-to-Noise ratio of the architecture several noise measurements were recorded as function of number of integrated pulses. Figure 8 shows the results.

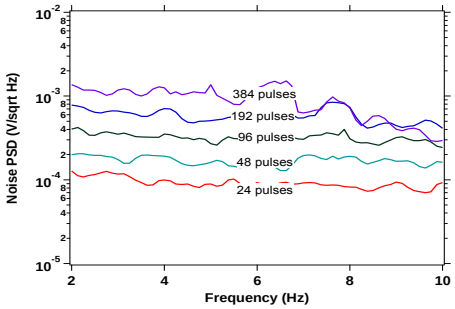

Fig. 8. Noise measurements vs. number of integrated pulses.

Integrating the measurements over the bandwidths of 100, 50, 25, 12.5 and 6.25Hz gives the transfer function of the noise as function of number of pulses. The trend is shown in figure 9.

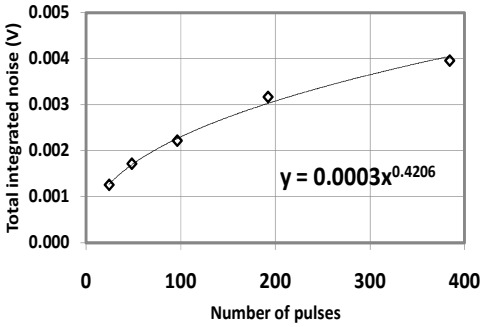

Fig. 9. Total integrated noise vs. number of pulses

The noise is proportional to $\sqrt{N}$, this has important implications. The signal-to-noise ratio benefits from this trend. The signal grows proportional to N while noise only grows as $\sqrt{N}$.

2.3 Benchmarking

The results of the measurements when compared to state-of-the-art devices are shown in table 1. The proposed architecture allows for a variable gain and extends the

bandwidth over other designs. Two figures of merit are quoted, mainly those used by Denison [6] and Paavola et al [7,8]. Each one focuses on different parameters to characterise accelerometer readouts. The developed readout is well placed among state-of-the-art devices when both metrics are used.

Table 1
State-of-the-art devices benchmarking

Parameter	Denison [6]	Paavola [7,8]	This work
Acceleration strain range	~±1g	±2g	±2.5g ±20,000με
Supply voltage	1.7-2.2V	1.0V	3.0V
Power	1.5μW	1.5μW	15μW
Noise Floor (accel.)	1mg/√Hz	704μg/√Hz	70μg/√Hz
Non-linearity	<1%	---	<1% [a] <0.6% [b]
Bandwidth	10Hz	1Hz	100Hz
FOM F√(W/Hz) μW·μg/Hz	8.1×10^{-22}	1400	4.41×10^{-20} 881
Technology	0.8μm CMOS	0.25μm CMOS	0.25μm CMOS
Area	----	2.25mm² [c]	2 mm² (active) 8 mm² [c]

[a] Acceleration
[b] Stress
[c] including ESD and I/O bondpads

As far as know to the authors the previous quotations to state-of-the-art devices are the most relevant ones in the literature and were selected to find a fair estimation to the proposed architecture. No references were found regarding strain sensors characterised for power efficiency. Nevertheless the values of this sensor are included in the benchmarking to highlight the advantages of this work over dedicated architectures [9,10].

2.4 Residual Motion

The accurate sin(x)/x transfer function of the amplifier allows the suppression of artefacts such as residual motion. Other known schemes such as that used by Hunter [4] require a resistor which usually is in the order of GW, therefore not knowing the precise 3dB point makes the suppression less efficient.

3. Conclusions

The paper shows the advantages of the presented architecture in terms flexibility for different types of sensors, control of SNR, bandwidth and gain.

State-of-the-art devices achieve excellent FOM because a dedicated architecture is developed for such devices where the sensitivity of the sensor is matched with the gain of the readout to obtain high efficiency. This work shows that a good FOM can be achieved without compromising versatility and even extending the range of the main parameters of certain applications.

Acknowledgements

The authors are grateful to Mikael Colin and Nicolas Bertsch from MEMSCAP for supplying the accelerator devices and their help in the measurements and interpretation of the data. Also we would like to express our gratitude to Nicolas Saillen from Thermo Fisher Scientific for the measurements of the strain sensor and extensive discussions.

References

[1] Suster. M. et al, " A High Performance MEMS Capacitive Strain Sensing System", *Journal of Microelectromechanical Systems*, vol. 15, no. 5, October 2006, pp. 1069-1077.

[2] Yi-Chen. C, Linear Programmable Switch-Capacitance Gain Amplifier, *US Patent No. 2008/0297243*, Dec.4, 2008.

[3] Weng. M. et al, "A High-Speed Low-Noise CMOS 16-Channel Charge-Sensitive Preamplifier ASIC for APD-Based PET Detectors", *IEEE Transactions on Nuclear Science*, Vol. 5, No. 4, August 2005, pp. 898-902.

[4] Hunter. S.R, Low Noise Radiation Sensor, *US Patent No. 2008/0122453*, May. 29, 2008.

[5] Boser. B and Howe. T., "Surface Micromachined Accelerometers", *IEEE Journal of Solid State Circuits*, vol. 31, no. 3, March 1996, pp. 366-375.

[6] Denison. T. et al, "A 2μW Three-Axis MEMS-based Accelerometer", *Instrumentation and Measurement Technology Conference,* IMTC 2007, Warsaw, Poland, May 1-3, 2007.

[7] Paavola. M. et al, "A Micropower ΔΣ-Based Interface ASIC for a Capacitive 3-Axis Micro-Accelerometer", *IEEE Journal of Solid-State Circuits*, vol. 44, no. 11, November 2009, pp. 3193-3210.

[8] Paavola. M, et al, "A 1.5μW 1V 2nd-order ΔΣ Sensor Front-End with Signal Boosting and Offset Compensation for a Capacitive 3-Axis Micro-Accelerometer", *ISSCC2008*, pp.577-579.

[9] ADXL330 Datasheet. "Small, Low Power, 3-Axis ±3g *i*MEMS Accelerometer", *Analog Devices*, Inc., 2007.

[10] Bracke. W et al, Generic architectures and design methods for autonomous sensors, *Sensors and Actuators A: Physical*. vol. 135, issue 2. April 2007, pp.881-888.